Colour changes by laser irradiation of reddish building limestones

C.M. Grossi[1] & D. Benavente[2]

1.- School of Health Sciences, University of East Anglia, Norwich NR4 7TJ, UK[1]

2.- Department of Earth and Environment Sciences. University of Alicante. 03690 Alicante (Spain)

Abstract

We have used X-ray photoelectron spectroscopy (XPS) as a novel method to investigate the causes of colour changes in a reddish limestone under irradiation by a Q-switched Nd:YAG 1064nm laser. We irradiated clean dry and wet surfaces of *Pidramuelle Roja,* a building stone frequently used in the Asturian heritage, at fluences ranging from 0.12 to 1.47 Jcm^{-2}. We measured the colour coordinates and undertook XPS analysis of the state of oxidation of iron both before and after irradiation. Visible colour changes and potential aesthetic damage occurred on dry surfaces from a fluence of 0.31 J cm^{-2}, with the stone showing a greening effect and very intense darkening. The colour change on dry surfaces was considerably higher than on wet surfaces, which at the highest fluence (1.47 J cm^{-2}) was also above the human visual detection threshold. The use of XPS demonstrated that the change in colour (chroma and hue) is associated with a reduction in the iron oxidation state on dry surfaces during laser irradiation. This points out to a potential routinary use of XPS to analyse causes of colour changes during laser cleaning in other types of coloured building stones.

Keywords: Q-switched Nd:YAG 1064nm laser, heritage red limestones, X-ray photoelectron spectroscopy, iron oxidation state, colour variation

[1] Corresponding author: c.grossi-sampedro@uea.ac.uk

Highlights

- This is the first time that XPS is used to determine the cause of colour change in coloured stones when cleaned with laser at 1064 nm
- We demonstrate that the colour change in red limestones is due to a reduction in the state of oxidation of iron, in this case present as hematite.
- XPS could be routinely used to analyse causes of colour changes during laser cleaning in other types of coloured building stones.

1. Introduction

The pulsed mode solid-state “Nd ions - Yttrium Aluminum Garnet” (Nd:YAG) laser at the fundamental wavelength of 1064 nm is a widely type of laser used for cleaning building stone. This type of laser is generally considered very suitable for stone cleaning because of its ability for the selective removal of dirt [1]. The chemical and mineralogical composition of the stones affects the absorption to laser radiation and therefore possible chemical and physical transformations and their concomitant colour-related change.

Colour is one of the stone characteristics that influence its use as building material. Changes in stone colour can be publicly acceptable but also aesthetically unpleasant [2]. Therefore colour is a property that is often measured when undertaking research in conservation, especially when using laser cleaning [3-13].

Colour changes are frequently measured using the CIELAB and CIELCH systems because they better represent human sensibility to colour than other colour coding systems. The variable L* represents lightness or luminosity, and a* (red-green) and b* (yellow-blue) are the chromatic coordinates. Chroma (C^*_{ab}: saturation or colour purity) and hue (h_{ab}: colour wheel) in the polar system CIELCH are calculated by the equations: $C^*_{ab} = (a^{*2} + b^{*2})^{1/2}$ and $h_{ab} = \tan^{-1}(b^*/a^*)$. Consequently, changes in C^*_{ab} and h_{ab} are more sensitive to changes on a* or b* depending on the original colour of the material [8].

Colour in most building stones is strongly influenced by the content, oxidation state and types of iron compounds. In general, colour changes are usually attributed to changes in the state of oxidation of iron [14-16]. Iron compounds are highly absorbent to 1064 nm laser radiation and therefore strongly condition the response of stone to laser irradiation, especially regarding to colour changes. In our previous research [7,8] we found that the a* coordinate, or red–green component, is strongly affected. Pink granites and reddish limestones, with higher positive a* values experienced large colour changes, mainly a decrease in a*, leading also to changes in h_{ab} (hue). Visually, red limestones stones turned into greener tones. We attributed changes in a* to thermal effects on the Fe_2O_3 likely contained in the rock minerals. However, we did not assess this experimentally.

Here we use X-ray photoelectron spectroscopy (XPS) as a novel method to investigate the causes of chemical variations leading to colour changes in a reddish limestone under laser irradiation at 1064 nm wavelength. The XPS technique has only been recently -and very rarely- used to analyse potential changes on stone surfaces by laser cleaning at different wavelengths [17,18]. One of the strengths of XPS is the identification of oxidation states [19] and it is widely used for quantitative analysis of surface chemical composition. The XPS detector quantifies the amount of photoelectrons emitted by the sample after being triggered with the X-ray source. Binding energy (BE) is related to the energy needed to extract the photoelectrons from the atom and is characteristic of each element and their oxidation state. Since core level electrons in solid-state atoms are quantized, the resulting energy spectra exhibits peaks characteristic of the electronic structure for atoms in the sample [20].

3. Materials and Methods

3.1. Material

In this investigation, we have used the reddish building stone *Piedramuelle Roja,* which is extensively used in historic buildings of Oviedo (Asturias, Northern-Spain), including the Cathedral and the Pre-Romanesque monuments. *Piedramuelle Roja* is a limestone with calcite and Fe-rich dolomite (70-80%), quartz (15-25%), and iron oxides (5%), mainly as goethite and hematite, which confer the colour to the stone. Muscovite, chlorite, glauconite and illite are minor components of this stone. Open porosity ranges from 5 to 15% and the mean value of pore throat size is circa 0.1 µm [6, 21].

3.2. Methods

3.2.1. Laser irradiation

Experiments were carried out using a Q-switching Nd:YAG laser system; λ= 1064 nm; spot diameter = 6 mm; pulse frequency rate = 20 Hz; pulse duration=6ns and maximum pulse energy varying around 353 – 415 mJ. Details of the method are described in Esbert et al., [6]. We irradiated clean stone samples as follows:

1. On dry surfaces (50 mm × 50 mm) at fluences ranging from 0.12 to 1.47 Jcm-2 along different strips. Each strip was irradiated five times.
2. On dry and wet surfaces (50 mm × 50 mm), applying a thin layer of water before laser irradiation, at two different fluences (0.5 and 1.47 J cm^{-2}).

3.2.2. Colour measurements

Colour was measured prior, and after irradiation with a MINOLTA CR-200 colorimeter using the illuminant C, beam of diffuse light of 8 mm diameter, 0º viewing angle geometry, specular component included and spectral response closely matching the CIE (1931) standard observer curves. A representative colour and reduced error because of colour variability was gained by using the differences between two successive cumulative averages of the parameters L*, a* and b*.

The CIELAB and CIELCH systems were used here to represent colour differences [EN ISO 105-J05, 22], and to compare the relative importance of each parameter in the colour change. We also refer to the total colour difference and an approximate corresponding grey scale rating (GSc) according to EN ISO 105-A05 [23]. Grey scale values indicate human visual discrimination to colour variation and vary from 5 (nonvisible changes) to 1 (very strong changes) and relate to intervals of ΔE^*_{94} from <0.40 to ≥11.60. Possible causes for colour changes were initially assessed by opaque minerals´ examination under reflected-light optical microscopy.

Descriptive statistics involved determination of means, standard errors and 95% confidence intervals. Statistical significance of the colour changes was evaluated by the Mann–Whitney (Wilcoxon rank) nonparametric test in STATA 14. Colour changes were plotted, for an easier visualisation, as polar and scatter plots.

3.2.3. XPS analysis

X-ray Photoelectron (XPS) provides information about the oxidation state of the elements and their concentration at the sample surface. A K-ALPHA XPS system (Thermo Scientific) was used to analyse the state of the oxidation of iron in the samples before and after laser irradiation. All spectra were collected using K-alpha radiation (1486.6 eV), yielding a focused X-ray spot with a diameter of 300 µm, at 3 mA and 12 kV. Twenty eight cumulative scans were performed in order to obtain an adequate signal-to-noise ratio. Differences between pre and post laser application were analysed by calculating odds ratios of the spectra peak´s height and area for Fe^{2+} vs Fe^{3+} and their 95% confidence intervals using STATA 14.

4. Results and discussion

4.1. Colour changes

The main colour changes are summarised in Figs. 1-3 and in Table 1. *Piedramuelle Roja* limestone is strongly affected by laser radiation, mainly when irradiated on dry surfaces. Fig. 1 shows colour changes (ΔE^*_{94}) and the equivalent grey scale rating (GSc) at different fluences on dry surfaces. Visual changes are detected from a fluence of 0.31 J cm^{-2}, with the stone showing a greening effect and very intense darkening. This changes are significant in L*, a* and b*. However, possible changes mainly in a* and perhaps b* could occur at lower fluences [see details in Esbert et al, 6].

Table 1 and Figures 2 and 3 show colour changes on tables irradiated at 1.47 J cm^{-2}. Colour change on wet surfaces is considerably lower but above the human visual detection threshold. *Piedramuelle Roja* limestone shows GSc values at 1.47 J cm^{-2} that evidence visual colour variations. Wet surfaces of the stones experience smaller but significant changes in L*, a* and b*. On wet surfaces, there is an increase in the b* co-ordinate that results in a subsequent increase in chroma.

Hematite, limonite and goethite were identified under reflectance microscopy in the untreated surfaces. After laser irradiation on dry surfaces, the stone orange background disappears and no hematite is clearly observed [see details in Esbert et al., 6].

4.2. Variation of the oxidation state of iron

The XPS analysis provided interesting information about oxidation sates of iron under different conditions. Table 2 and Figure 4 show the region of the spectrum corresponding to high-resolution iron $2p_{3/2}$ XPS transitions for the iron species in untreated and laser-irradiated *Piedramuelle Roja* dry surfaces. The spectra deconvolution is produced since they are clearly separated by about 1.2 eV and with ½ intensity ratios between them [24]. Each deconvoluted peak is a 30% mixed Lorentzian/Gaussian function. The obtained deconvolution of the iron $2p_{3/2}$ spectra shows three main peaks.

Peak A occurs at a binding energy (BE) about 709 eV, peak B at 711 eV and peak C at 714 eV. The low-BE (peak A) corresponds to ferrous (Fe^{2+}) compounds and the main peak in the centre of spectra (peak B) includes the ferric (Fe^{3+}) compounds. The high-BE peak (peak C) is assigned to a surface or satellite peak, which has been ascribed to shake-up or charge transfer processes [20,25-28]. Consequently, the evolution of oxidation state of iron compounds is studied through the peaks A and B.

We used the binding energy of the deconvoluted peaks to analyse the evolution of oxidation state of iron compounds. The binding energy values of these peaks significantly changed by laser irradiation, although their values slightly decrease to the reduce form (Table 2).

The intensity has been defined as both height and area ratios of the peaks A and B (A/B). This means that laser irradiation produces a reduction of the oxidised iron, which is presented in *Piedramuelle Roja* minerals mainly as hematite. Thus, the A/B height and area ratios (Fe^{2+}/Fe^{3+} compounds) tend to increase after laser irradiation, which seems to be significant as there is not overlapping between the 95% CI pre and post laser (Table 2). Odds ratios Fe^{2+} vs Fe^{3+} for height and area post vs pre laser are significant higher than 1, with 95% CI both lower and upper bounds higher than 1. Height and area odds ratios are very similar, around 1.4 (95%CI 1.3-1.5) suggesting an increase in the odds of Fe^{2+} of around 40% after laser irradiation at this experimental conditions.

5. Conclusions

The analysis carried out by XPS proved that iron reduction is the main responsible of colour changes on dry surfaces of *Piedramuelle Roja* limestone irradiated with laser at 1064 nm, i.e. at absorbing near-red wavelengths. As iron is the element that has the strongest influence on the colour of limestone, this is translated in strong visible colour changes (hue and chroma), statistically significant in all colour coordinates, with the a*coordinate (red-green) being especially sensitive.

Visible colour changes and potential aesthetic damage occurred on dry surfaces from a fluence of 0.31 J cm^{-2}, with the stone showing a greening effect and very intense darkening. The colour change on dry surfaces is considerably higher than on wet surfaces, which at the highest fluence (1.47 J cm^{-2}) is also above the human visual detection threshold.

XPS could be routinary used to analyse causes of colour changes during laser cleaning in other type of coloured building stones.

Acknowledgements

This research was partially funded by the Royal Society Joint grant scheme (UK) and the CICYT (Spain), contract grant number 1FD97-0331-C03-01. We would like to dedicate this document to our dear Prof. Rosa M. Esbert.

References

1. M. Cooper, Laser Cleaning in Conservation, An Introduction, Butterworth-Heinemann, Oxford, 1998.
2. C. Andrew, Towards an aesthetic theory of building soiling, in Stone Cleaning and the Nature, Soiling and Decay Mechanisms of Stone, Donhead: London, 1992; pp 63-81.
3. J.M. Lee, W.M. Steen, In-process surface monitoring for laser cleaning processes using a chromatic modulation technique, Int. J. Adv. Manuf. Tech.17 (2001) 281–287.
4. S. Klein, F. Fersanki, J. Hildenhagen, K. Dickmann, H. Uphoff, Y. Marakis, V. Zafiropolous, Discoloration of marble during laser cleaning by Nd:YAG laser wavelengths, App. Surf. Sci. 171 (2001) 242–251.

5. D. Eichert, V. Vergès-Belmin, O. Kahn, Electronic paramagnetic resonance as a tool for studying the blackening of Carrara marble due to irradiation by Q-switched YAG laser, J. Cult. Herit. 1 (2000) S37–S45.
6. R.M. Esbert, C.M. Grossi, A. Rojo, F.J. Alonso, M. Montoto, J. Ordaz, C. Pérez de Andrés, C. Escudero, M. Barrera, E. Sebastián, C. Rodríguez-Navarro, K. Elert, Application limits of Q-switched Nd:YAG laser irradiation for stone cleaning based on colour measurements, J. Cult. Herit. 4 (2003) S50s–S55s.
7. C.M. Grossi, F.J. Alonso, R.M. Esbert, A. Rojo, Effect of Laser Cleaning on Granite Color, Color Res. Appl. 32 (2007) 152 – 159.
8. C.M. Grossi, P. Brimblecombe, R.M. Esbert, F.J. Alonso, Color Changes in Architectural Limestones from Pollution and Cleaning, Color Res. Appl. 32 (2007) 320-331.
9. J. Delgado Rodrigues, D. Costa, M. Marcalchi, I. Osticioli, S. Siano, Laser ablation of iron-rich black films from exposed granite surfaces, App. Phys. A 117 (2014) 365-370.
10. T. Rivas, S. Pozo, M.P. Fiorucci, A.J. López, A. Ramil, Nd:YVO_4 laser removal of graffiti from granite, influence of Paint and rock properties on cleaning efficacy, Appl. Surf. Sci. 263 (2012) 563-572.
11. P. Ortiz, V. Antúnez, R. Ortiz, J.M. Martín, M.A. Gómez, A.R. Hortal, B. Martínez-Haya, Comparative study of pulsed laser cleaning applied to weathered marble surfaces, Appl. Surf. Sci. 28 (2013) 193-201.
12. S. Pozo, P. Barreoro, T. Rivas, P. González, M.P. Fiorucci, Effectiveness and harmful effects of removal sulphated black crust from granite using Nd:YAG nanosecond pulsed laser, Appl. Surf. Sci. 302 (2014) 309-313.
13. M. Lettieri, M. Masieri, Surface characterization and effectiveness evaluation of anti-graffiti coatings on highly porous stone materials, Appl. Surf. Sci. 288 (2014) 466-477.

14. S. Siano, F. Fabiani, R. Pini, R. Salimbeni, M. Giamello, G. Sabatini, Determination of damage threshold to prevent side effects in laser cleaning of Pliocene sandstone of Siena, J. Cult. Herit. 1 (2000) S47–S53.
15. M. Labouré, P. Bromblet, G. Orial, P. Wiedemann, C. Simon-Boisson, Assessment of laser cleaning on limestones and sandstones, J. Cult. Herit. 1 (2000) S21–S27.
16. D. Eichert, V. Vergès-Belmin, O. Kahn, Electronic paramagnetic resonance as a tool for studying the blackening of Carrara marble due to irradiation by Q-swithched YAG laser, J. Cult. Herit. 1 (2000) S37– S45.
17. C.M. Grossi, D. Benavente, R.M. Esbert, F.J. Alonso, P. Brimblecombe, M.A. García-del-Cura, Analysis of colour changes by laser irradiation of reddish building limestone using X-ray photoelectron spectroscopy, Lacona VII, Madrid, 2007, 129.
18. A.J. López, T. Rivas, J. Lamas, A. Ramil, A. Yáñez, Optimisation of laser removal of biological crusts in granites, Appl Phys A 100 (2010) 733-739.
19. J.B. Lambert, C.D. McLaughlin, C.E. Shawl, L. Xue, X-ray photoelectron spectroscopy and archaeology, Anal. Chem. 71 (1999) 614A-620A.
20. P. Vazquez, M. Acuña, D. Benavente, S. Gibeaux, I. Navarro, M. Gomez-Heras, Evolution of surface properties of ornamental granitoids exposed to high temperatures, 104 Constr. Build. Mater. (2016) 263-275.
21. F.J. Alonso, J. Ordaz, L. Valdeón, A. Rojo, F. Díaz-Pache, R.M. Esbert, Caracterización Petrofísica de la caliza de Piedramuelle (Oviedo, Asturias), Trabajos de geología. Universidad de Oviedo, 21 (1999) 25-31.
22. EN ISO 105-J03, Textiles – Tests for Colour Fastness. Part J03. Calculation of Colour Differences, 1997
23. EN ISO 105-A05, Textiles – Tests for Colour Fastness. Part A05. Instrumental Assessment of Change of Colour for Determination of Grey Scale Rating, 1997.

24. J.F. Moulder, J. Chastain, W.F. Stickle, P.E. Sobol, K.D. Bomben, Handbook of Xray photoelectron spectroscopy: a reference book of standard spectra for identification and interpretation of XPS data, Physical Electronics, Eden Prairie, 1995.
25. L. Yin, I. Adler, T. Tsang, L.J. Matienzo, S.O. Grim, Paramagnetism and shake-up satellites in X-ray photoelectron spectra, Chem. Phys. Lett. 24 (1974) 81–84.
26. C. Mustin, Ph. De Donato, R. Benoit, R. Erre, Spatial distribution of iron and sulphur species on the surface of pyrite, Appl. Surf. Sci. 68 (1993) 147–158.
27. B.S. Norgren, M.A.J. Somers, J.H.W. de Wit, Application of Tougaard background subtraction to XPS spectra of passivated Fe-17 Cr, Surf. Interface Anal. 21 (6-7) (1994) 378–381.
28. A.P. Grosvenor, B.A. Kobe, M.C. Biesinger, N.S. McIntyre, Investigation of multiplet splitting of Fe 2p XPS spectra and bonding in iron compounds, Surf. Interface Anal. 36 (2004) 1564–1574.

	L*	a*	b*	C^*_{ab}	h_{ab}	ΔE^*_{94}	GSc
PRE DRY	59.1 (58.7-59.6)	11.9 (11.6-12.2)	21.5 (20.9-22.1)	24.6 (23.9-25.2)	60.9 (60.4-61-4)		
POST DRY	54.0 (53.6-54.4)	4.4 (4.2-4.6)	15.0 (14.7-15.4)	15.6 (15.3-16.0)	73.7 (73.2-74.3)	11.2(10.9-11.4)	1.5
p-value*	<0.001	<0.001	<0.001				
PRE WET	59.2 (58.8-59.5)	12.2 (11.9-12.4)	20.1 (19.8-20.5)	23.5 (23.2-23.9)	58.9 (58.5-59.3)		
POST WET	57.2 (57.0-57.5)	11.2 (11.0-11.3)	21.5 (21.4-21.7)	24.3 (24.1-24.4)	62.6 (62.2-63.0)	2.6 (2.6-2.6)	3.5
p-value*	<0.001	<0.001	<0.001				

* From Mann–Whitney (Wilcoxon rank) test

Table 1.- Mean and 95% confidence intervals of colour variables pre and post laser irradiation at 1.47 J cm^{-2} on dry and wet *Piedramuelle Roja* surfaces and colour changes (ΔE^*_{94} and GSc) measured following EN ISO recommendations [22, 23].

	Pre-laser	Post-laser
Energy (eV)		
Peak A (Fe^{+2})	709.9	709.83
Peak B (Fe^{+3})	711.89	711.53
Peak C (Satellite)	714.25	713.31
A/B height ratio	0.81 (0.79-0.83)	1.14 (1.12-1.15)
A/B area ratio	0.68 (0.67-0.69)	0.93 (0.92-0.94)
	Odds Ratio Post-laser vs Pre-laser	
Height Fe^{+2} vs Fe^{3+}	1.41 (1.29-1.54)	
Area Fe^{+2} vs Fe^{3+}	1.37 (1.30-1.45)	

Table 2.- Change in the Energy of $2p_{3/2}$ XPS Fe-peaks on *Piedramuelle Roja* surface pre and post Nd:YAG laser irradiation at 1064 nm wavelength on dry surfaces. In brackets 95% confidence intervals. Odds ratios and confidence intervals were calculated on 28 cumulative scan counts.

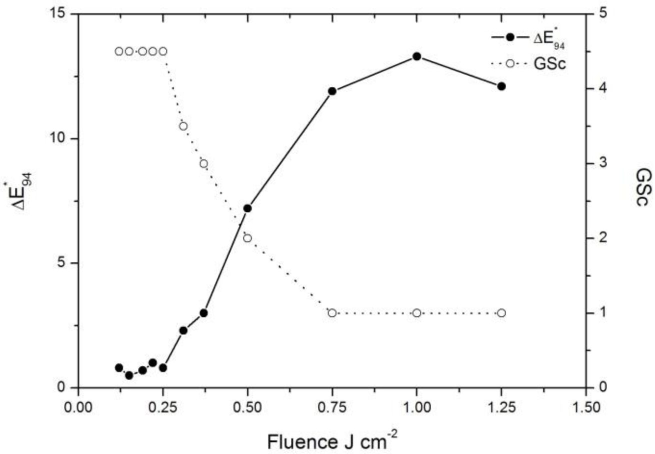

ΔE^*_{94}
GSc
Fluence J cm^{-2}
0
5
10
15
0
1
2
3
4
5
0.00
0.25
0.50
0.75
1.00
1.25
1.50

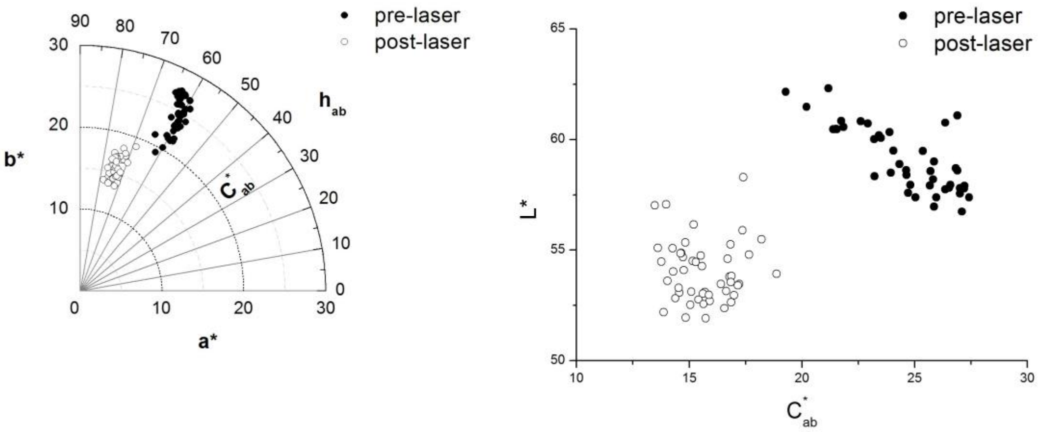
pre-laser
post-laser
b*
a*
h
ab
C*ab
L*
C*ab

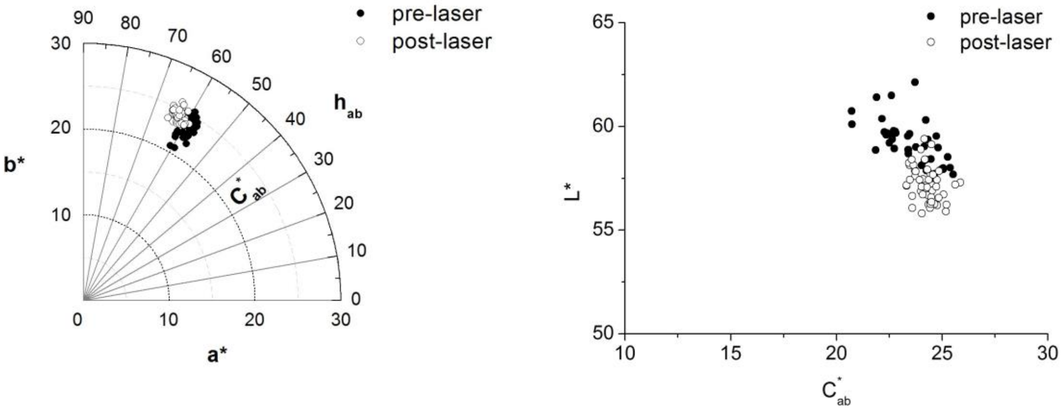
pre-laser
post-laser
b*
a*
h_ab
C*_ab
L*
C*_ab

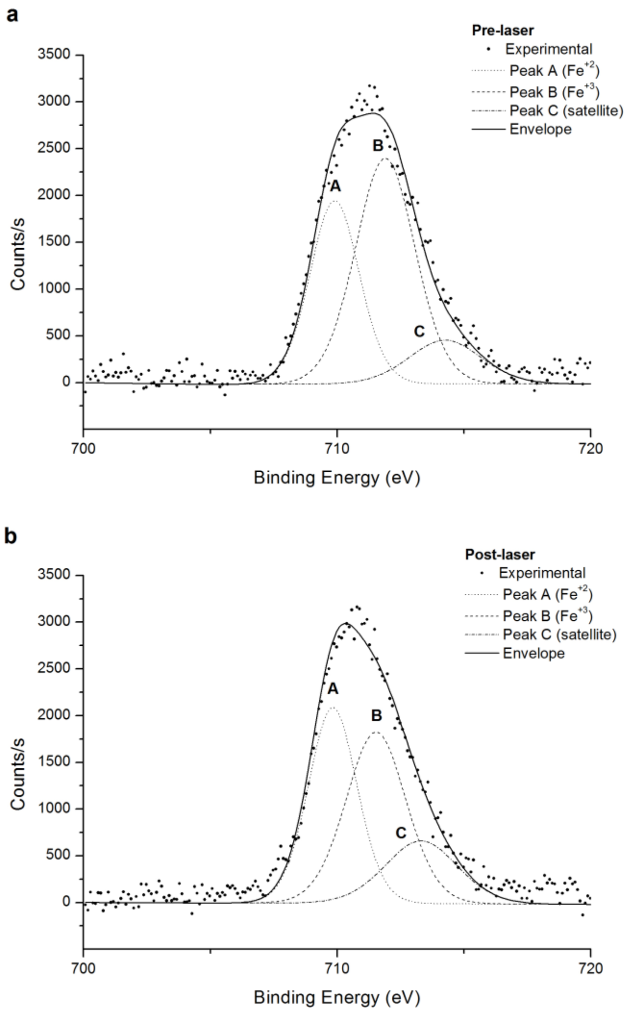
a
Pre-laser
Experimental
Peak A (Fe+2)
Peak B (Fe+3)
Peak C (satellite)
Envelope
A
B
C
Counts/s
Binding Energy (eV)
b
Post-laser
Experimental
Peak A (Fe+2)
Peak B (Fe+3)
Peak C (satellite)
Envelope
A
B
C
Counts/s
Binding Energy (eV)

Fig. 1. Colour changes (ΔE^*_{94}) and grey scale rating (GSc) at different fluences on dry surfaces of *Piedramuelle Roja* [EN ISO 105-A05, 24].

Fig. 2. Polar and Cartesian scattergrams for *Piedramuelle Roja* limestone irradiated with Q-switched Nd:YAG 1064nm laser at 1.47 J cm^{-2} on dry surfaces [8].

Fig. 3. Polar and Cartesian scattergrams for *Piedramuelle Roja* limestone irradiated with Q-switched Nd:YAG 1064nm laser at 1.47 J cm^{-2} on wet surfaces.

Fig. 4: Evolution of Fe $2p_{3/2}$ XPS spectrums for *Piedramuelle Roja* limestone pre (a) and post (b) irradiation with Q-switched Nd:YAG 1064nm laser on dry surfaces.